Global Journal of Pure and Applied Mathematics.
ISSN 0973-1768 Volume 13, Number 9 (2017), pp. 4851-4867

http://www.ripublication.com

Irreversibility Analysis of MHD Mixed Convection Channel Flow of Nanofluid with Suction and Injection

O. D. Makinde* and M.S. Tshehla

Faculty of Military Science, Stellenbosch University,
Private Bag X2, Saldanha 7395, South Africa.

**Corresponding Author*

Abstract

The inherent irreversibility in hydromagnetic mixed convection channel flow of Cu-water nanofluid in the presence of suction and injection at the walls. In addition, the entropy production decreased at the permeable walls but increased at the channel core region with a rise in magnetic field intensity. Investigated theoretically based on first and second laws of thermodynamics. The model equations of momentum and energy balance are obtained and tackled numerically using a shooting technique coupled with a fourth order Runge-Kutta-Fehlberg integration scheme. The results obtained for the velocity and temperature profiles are utilised to determine the skin friction, Nusselt number, entropy generation rate and Bejan number. The results reveal that the enhancement of the Nusselt number due to presence of Cu-nanoparticles increases the magnitude of entropy generation and Bejan number. In addition, the entropy production is decreased at the permeable walls but increased at the channel core region with a rise in magnetic field intensity.

Keywords: MHD; Channel flow; Mixed convection; Nanofluid; Entropy analysis; Suction/Injection

Nomenclature

(u, v) velocity components	β_{nf} nanofluid thermal expansion coefficient
(x, Y) coordinates	β_{bf} base fluid thermal expansion coefficient
k_{nf} nanofluid thermal conductivity	β_p solid thermal expansion coefficient
Pr Prandtl number	α_{nf} nanofluid thermal diffusivity
C_f skin friction coefficient	σ_{nf} nanofluid electrical conductivity
V suction/injection velocity	ρ_{nf} nanofluid density
Br Brinkmann number	ρ_p solid fraction density
w dimensionless axial velocity	ρ_f base fluid density
T temperature	υ_f base fluid kinematic viscosity
k_p solid fraction thermal conductivity	μ_{nf} nanofluid dynamic viscosity
Re suction/injection Reynolds number	μ_f base fluid dynamic viscosity
k_f base fluid fraction thermal conductivity	ϕ solid volume fraction parameter
Ha Hartmann number	θ dimensionless temperature
C_{pp} nanopartcles specific heat	Ω temperature difference parameter
C_{pf} base fluid specific heat	
C_{pnf} nanofluid specific heat	
Nu Nusselt number	
Be Bejan number	
Ns entropy generation rate	

Greek symbols

INTRODUCTION

Studies related to mixed convection flow of hydromagnetic nanofluid through a channel with permeable walls have attracted the attention of many researchers due to their numerous engineering and industrial applications, particularly as a control mechanism in material manufacturing, micro MHD pumps, micromixing of physiological samples, biological transportation, heat exchanger, drug delivery, solidification process in metallurgy and in some astrophysical problems [1]. For a mixed convection of an electrically conducting nanofluid exposed to a magnetic field, the Lorentz force is very active and can be used to regulate a variety of flow regimes by interacting with the buoyancy force in governing the flow and temperature fields [2]. Nanofluid as described by Choi [3] in his pioneering work is a colloidal suspension of metallic or non-metallic nanometer sized particles dispersed uniformly into conventional base fluids. Nanofluid shows a significant improvement in the heat transfer performance as compared to the conventional base fluid like ethylene glycol, water and engine oil [4]. The magnetic nanofluids possess both liquid and magnetic properties. The advantage of magnetic nanofluid is that fluid flow and heat transfer can be controlled by external magnetic field, which makes it applicable in various fields such as electronic packing, thermal engineering and aerospace [5]. The

hydromagnetic bioconvection in conducting nanofluid flow with nonlinear thermal radiation and quartic autocatalysis chemical reaction past an upper surface of a paraboloid of revolution was addressed by Makinde and Animasaun [6]. A numerical study of the effects of magnetic field on nanofluid forced convection in a partially heated microchannel was conducted by Aminossadati *et al.* [7]. The combined effects of Newtonian heating and magnetic field on free convective flow of an electrically conducting nanofluid over a stationary flat surface was numerically examined by Uddin *et al.* [8].

Meanwhile, the analysis of inherent irreversibility in nanofluid flow and heat transfer is currently one of the important issues in many engineering and industrial processes involving continuous exchange of kinetic energy to heat energy. This is clearly revealed through the application of second law of thermodynamics. Entropy generation measures the destruction of the available work of a system and is closely related to the thermodynamics irreversibility. The determination of the various factors responsible for the entropy generation is also important in upgrading the system performances. Theoretical study on entropy generation in fluid flow and heat transfer problem was pioneered by Bejan [9]. Thereafter, several authors have investigated the problem of fluid flow irreversibility under various flow physical situations [10-15]. A numerical study of heat transfer and entropy generation of natural circulation in a square cavity filled with Al_2O_3 nanofluid was performed by Cho [16]. Leong *et al*. [17] analysed the heat transfer and entropy generation in three different types of heat exchangers operated with nanofluids. Mahmoudi *et al*. [18] numerically investigated the effects of magnetic field on entropy generation and enhancement of heat transfer in a trapezoidal enclosure with Copper (Cu)–water nanofluid. It was observed that the entropy generation is decreased when the nanoparticles are present, while the magnetic field generally increases the magnitude of the entropy generation. To the best of authors' knowledge, the combined effects of buoyancy force, suction/injection, magnetic field, viscous and Joule heating no inherent irreversibility in hydromagnetic nanofluid has been reported in the literature yet. Therefore, the present article deals with the second law analysis due to mixed convection in a vertical channel with permeable walls filled by Cu-water nanofluid in the presence of a magnetic field. The viscosity of the nanofluid used is that of Brinkman [19] and the effective electrical conductivity is that proposed by Maxwell [20]. The model equations of momentum and energy balance are obtained and the numerical solutions are developed for various values of embedded parameters using a shooting technique coupled with a fourth order Runge-Kutta-Fehlberg integration scheme [21]. Graphical results are discussed to deeply understand the physics of the problem.

2. MATHEMATICAL FORMULATION

We consider the hydromagnetic flow of an electrically conducting incompressible Cu-Water nanofluid in a vertical channel having permeable walls as shown in figure 1. The flow is in the direction of *x*-axis and the *y*-axis is taken perpendicular to it. The flow field is exposed to the influence of an external, transversely applied, uniform magnetic field of strength B_0. The magnetic Reynolds number and the induced electric field are assumed to be small and negligible. The channel width is denoted by *h* with uniform temperature T_0 at Y=0 and temperature T_1 at Y= *h* such that $T_0 < T_1$. The volume fraction of the Cu-nanoparticles in the base fluid (water) is taken to be from 0 to 10% (i.e. ϕ = 0 to 0.1) and assumed to have been mixed homogeneously with the base fluid under laboratory condition thus we have a single phase flow.

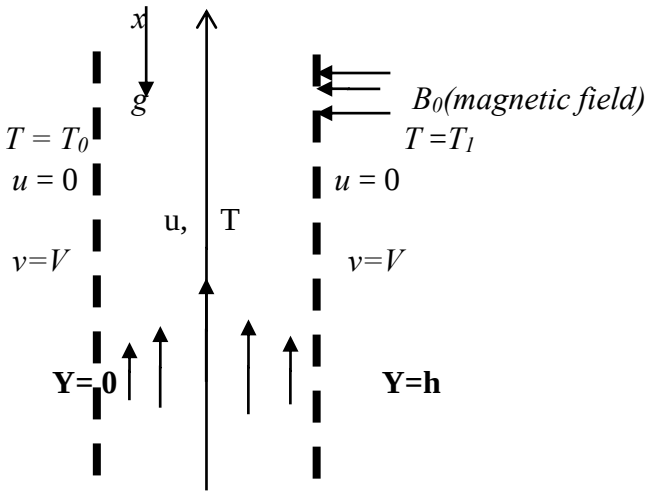

Figure 1. Physical model of the problem.

Using the Boussinesq approximation for the buoyancy term and under the above assumptions, the governing equations for the momentum and energy balance can be expressed as [6, 7, 10, 15, 16, 18];

$$\left.\begin{aligned} &-V\frac{du}{dY}+\beta_{nf}g\left(T-T_0\right)-\frac{1}{\rho_{nf}}\frac{dP}{dx}+\frac{\mu_{nf}}{\rho_{nf}}\frac{d^2u}{dY^2}-\frac{\sigma_{nf}B_0^2u}{\rho_{nf}}=0,\\ &-\left(\rho C_p\right)_{nf}V\frac{dT}{dY}+k_{nf}\frac{d^2T}{dY^2}+\mu_{nf}\left(\frac{du}{dY}\right)^2+\sigma_{nf}B_0^2u^2=0,\\ &E_g=\frac{k_{nf}}{T_0^2}\left(\frac{dT}{dY}\right)^2+\frac{\mu_{nf}}{T_0}\left(\frac{du}{dY}\right)^2+\frac{\sigma_{nf}B_0^2}{T_0}u^2, \end{aligned}\right\} \quad (1)$$

with the following boundary conditions

$$\left.\begin{aligned} u(0) = u(h) = 0, \\ T(0) = T_0, T(h) = T_1, \end{aligned}\right\} \tag{2}$$

where u is the axial velocity, P is the pressure, x is the axial distance, ρ_{nf} is the nanofluid density, μ_{nf} is the nanofluiddynamic viscosity, C_{pnf} is the nanofluid specific heat capacity at constant pressure, k_{nf} is the nanofluid thermal conductivity, E_g is the entropy generation rate, T is the nanofluid temperature, σ_{nf} is the nanofluid electrical conductivity, g is the gravitational acceleration and β_{nf} is the nanofluid thermal expansion coefficient. In equation (1), the Cu-water nanofluid thermophysical properties are given by [16-20]

$$\rho_{nf} = (1-\phi)\rho_{bf} + \phi\rho_p, (\rho C_p)_{nf} = (1-\phi)(\rho C_p)_{bf} + \phi(\rho C_p)_p, (\rho\beta)_{nf} = (1-\phi)(\rho\beta)_{bf} + \phi(\rho\beta)_p,$$
$$\frac{k_{nf}}{k_{bf}} = \frac{(k_p + 2k_{bf}) - 2\phi(k_{bf} - k_p)}{(k_p + 2k_{bf}) + \phi(k_{bf} - k_p)}, \sigma_{nf} = \sigma_{bf}\left[1 + \frac{3(\gamma - 1)\phi}{(\gamma + 2) - (\gamma - 1)\phi}\right], \gamma = \frac{\sigma_P}{\sigma_{bf}}, \mu_{nf} = \frac{\mu_{bf}}{(1-\phi)^{2.5}}. \tag{3}$$

Table 1: Thermophysical properties of water and Cu nanoparticles [16-20]

Materials	ρ(kg/m^3)	C_p (J/kgK)	k (W/mK)	σ(S/m)	$\beta x10^5(K^{-1})$
Pure water	997.1	4179	0.613	5.5x10^{-6}	21
Copper (Cu)	8933	385	401	59.6x10^6	1.67

where ρ_{bf} is the base fluid density, ρ_p is the nanoparticles density, μ_{bf} is the base fluid dynamic viscosity, k_{bf} is the basefluid thermal conductivity, k_p is the nanoparticles thermal conductivity, β_{bf} is the base fluid thermal expansion coefficient, β_p is the nanoparticles thermal expansion coefficient, C_{pbf} is the base fluid specific heat capacity, C_{pp} is the nanoparticles specific heat capacity, σ_{bf} is the base fluid electrical conductivity and σ_p is the nanoparticles electrical conductivity. Introducing the following dimensionless parameters and variables,

$$w=\frac{uh}{\upsilon_{bf}},\ Gr=\frac{g\beta_{bf}(T_1-T_0)h^3}{\upsilon_{bf}^2},\ \Pr=\frac{(\mu C_p)_{bf}}{k_{bf}},\ Ha^2=\frac{\sigma_{bf}B_0^2h^2}{\mu_{bf}},\ y=\frac{Y}{h},\ L=\frac{d\overline{P}}{dX},$$

$$Br=\frac{\mu_{bf}\upsilon_{bf}^2}{k_{bf}(T_1-T_0)h^2},\ A_1=Q\left[1+\frac{3(\gamma-1)\phi}{(\gamma+2)-(\gamma-1)\phi}\right],\ Q=(1-\phi)^{2.5},\ \theta=\frac{T-T_0}{T_1-T_0},$$

$$M=\frac{(k_p+2k_{bf})+\phi(k_{bf}-k_p)}{(k_p+2k_{bf})-2\phi(k_{bf}-k_p)},\ \overline{P}=\frac{Ph^2\rho_{bf}}{\mu_{bf}^2},\ \mathrm{Re}=\frac{Vh}{\upsilon_{bf}},\ Ec=\frac{\upsilon_{bf}^2}{C_{pbf}(T_1-T_0)h^2},$$

$$A_3=Q\left[1-\phi+\phi\frac{(\rho\beta)_p}{(\rho\beta)_{bf}}\right],\ A_4=\frac{M}{Q},\ A_5=M\left[1+\frac{3(\gamma-1)\phi}{(\gamma+2)-(\gamma-1)\phi}\right],\ Ns=\frac{h^2E_gT_0^2}{k_{bf}(T_1-T_0)^2},$$

$$A_2=Q\left[1-\phi+\phi\frac{\rho_p}{\rho_{bf}}\right],\ A_6=M\left[1-\phi+\phi\frac{(\rho C_p)_p}{(\rho C_p)_{bf}}\right],\ X=\frac{x}{h},\upsilon_{bf}=\frac{\mu_{bf}}{\rho_{bf}},\gamma=\frac{\sigma_p}{\sigma_{bf}},$$

(4)

and we obtain

$$\left.\begin{aligned}\frac{d^2w}{dy^2}&=A_2\,\mathrm{Re}\frac{dw}{dy}+A_1Ha^2w-A_3Gr\theta-QL, \qquad w(0)=w(1)=0,\\ \frac{d^2\theta}{dy^2}&=A_6\,\Pr\mathrm{Re}\frac{d\theta}{dy}-A_4Ec\,\Pr\left(\frac{dw}{dy}\right)^2-A_5Ec\,\Pr Ha^2w^2, \quad \theta(0)=0,\theta(1)=1,\end{aligned}\right\} \tag{5}$$

where *Pr* is the Prandtl number, *Ha* is the Hartmann number, *Ec* is the Eckert number, *Gr* is the Grashof number, *Re* is the wall suction/ injection parameter, and *L* is the axial pressure gradient parameter. Using equation (4), the dimensionless form of the entropy generation rate expression is obtained as [9, 18];

$$Ns=\frac{1}{M}\left(\frac{d\theta}{dy}\right)^2+\frac{Br}{\Omega Q}\left[\left(\frac{dw}{dy}\right)^2+A_1Ha^2w^2\right], \tag{6}$$

where $Br = EcPr$ is the Brinkman number, $\Omega = (T_1\text{-}T_0)/T_0$ is the temperature difference parameter and $Br\Omega^{-1}$ is group parameter. Let

$$N_1=\frac{1}{M}\left(\frac{d\theta}{dy}\right)^2,\ N_2=\frac{Br}{\Omega Q}\left[\left(\frac{dw}{dy}\right)^2+A_1Ha^2w^2\right],\ \lambda=\frac{N_2}{N_1}, \tag{7}$$

then, N_1 is the heat transfer irreversibility while N_2 is the irreversibility due to combined effects of fluid friction and magnetic field. The parameter λ represents the irreversibility ratio. The Bejan number (Be) that represents the ratio of the heat transfer irreversibility to the total entropy generation is given as

$$Be = \frac{N_1}{N_1 + N_2} = \frac{1}{1+\lambda}. \tag{8}$$

The skin friction (C_f) and the local Nusselt number (Nu) at the walls can be expressed as:

$$\left.\begin{aligned} C_f &= \frac{\rho_{bf} h^2 \tau_w}{\mu_{bf}^2} = \frac{1}{(1-\phi)^{2.5}} \left.\frac{du}{dy}\right|_{y=0,1} \\ Nu &= \frac{h q_w}{k_{bf} T_w} = -\frac{1}{M} \left.\frac{d\theta}{dy}\right|_{y=0,1} \end{aligned}\right\} \tag{9}$$

where τ_w and q_w are the wall shear stress and the heat flux at Y = 0 and h respectively and they are given as

$$\tau_w = \mu_{nf} \frac{du}{dY},\ q_w = -k_{nf} \frac{dT}{dY},\ \text{at } Y = 0,\ h. \tag{10}$$

3. NUMERICAL APPROACH

The dimensionless model equations (5) together with the boundary conditions represent a boundary value problem (BVP) and are transformed into a set of nonlinear first order ordinary differential equations with some unknown initial conditions to be determined by shooting technique. Let,

$$w = z_1\ , w' = z_2, \theta = z_3\ , \theta' = z_4. \tag{11}$$

The governing equations then become

$$\left.\begin{aligned} z_1' = z_2, z_2' &= A_2 \operatorname{Re} z_2 + A_1 Ha^2 z_1 - A_3 Grz_3 - QL \\ z_3' = z_4, z_4' &= A_6 \operatorname{Pr}\operatorname{Re} z_4 - A_4 Ec \operatorname{Pr} z_2^2 - A_5 Ec \operatorname{Pr} Ha^2 z_1^2 \end{aligned}\right\}, \tag{12}$$

with the corresponding initial conditions as

$$z_1(0) = 0, z_2(0) = a_1, z_3(0) = 0\ , z_4(0) = a_2. \tag{13}$$

We determined the appropriate values of the unknown initial conditions a_1, a_2 using Newton-Raphson's method for each set of parameter values after the first guess. A fourth order Runge-Kutta-Fehlberg integration scheme is then implemented with the step size Δy=0.01 in order to numerically tackle the obtained initial value problem [21]. From the process of numerical computation, we obtain the skin friction (C_f), the Nusselt number (Nu), the entropy generation rate (Ns) and the Bejan number (Be) as given by equations (6)-(9).

4. RESULTS AND DISCUSSION

Numerical calculations are carried out for different thermophysical parameters controlling the flow and heat transfer with Cu-Water as working fluid. The Prandtl number for the base fluid (water) is taken as Pr= 6.2 [18] while the flow constant axial pressure parameter is taken as L = 1. Figures (2a)-(2d) depict the effects of nanoparticles volume fraction ϕ in the range of $0 \leq \varphi \leq 0.1$ on the fluid velocity, temperature, entropy generation rate and Bejan number. Generally, the velocity profile is zero at the walls due to prescribe no slip condition and attained its pick value within the channel. The nanofluid temperature is minimum the left wall and maximum at the right wall satisfying the prescribed boundary conditions. Interestingly, the conventional base fluid (water) flow faster with lower entropy generation rate and Bejan number as compared with that of Cu-water nanofluid. As the added Cu-nanoparticles volume fraction increases, a decrease in velocity profile and a slight increase in the temperature profile are observed. This may be attributed to a slight increase in the base fluid viscosity due to the presence of nanoparticles leading to decrease in the flow rate as shown in figure (2a). However, an increase in the inter-particles collision within the flow enhances the internal heat generation leading to a slight increase in nanofluid temperature within the channel as observed in figure (2b). Meanwhile, it is interesting to note that addition of nanoparticles to base fluid enhances both the entropy production and Bejan number as illustrated in figures (2c)–(2d). The addition of nanoparticles increases the irreversibility due to heat transfer increases and dominates the entropy generation in the flow system.

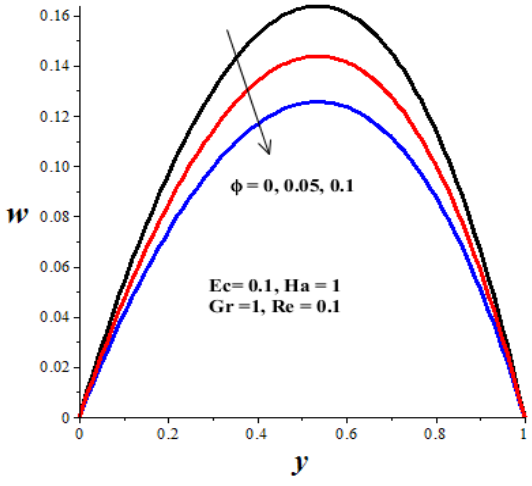

2a

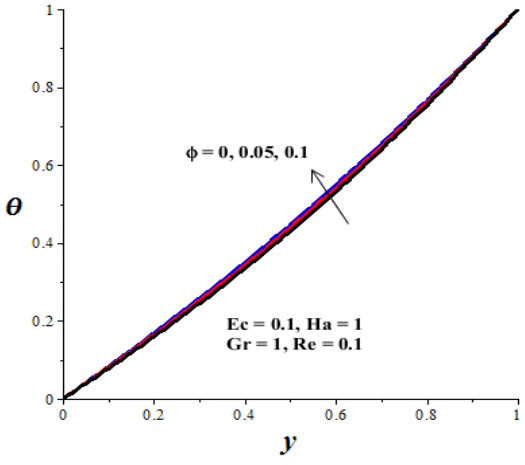

2b

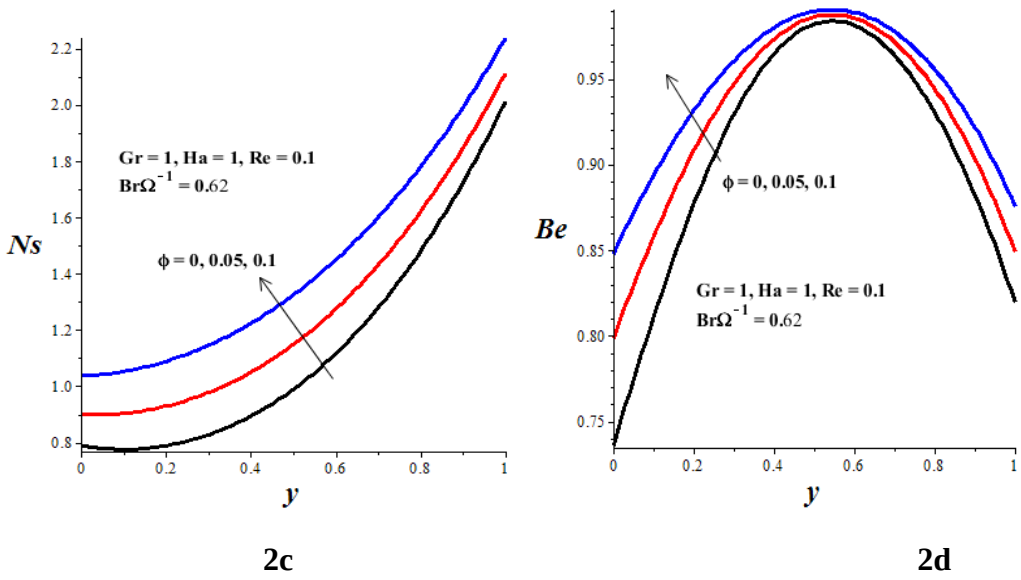

2c **2d**

Figure 2: Effect of Cu nanoparticles volume fraction on a) velocity, b) temperature c) entropy generation rate, d) Bejan number

The effects of suction/injection Reynolds number (*Re*) on the nanofluid velocity, temperature, entropy generation rate and Bejan number are displayed in figures (3a)-(3d). It is observed that both velocity and temperature profiles decrease with an increase in nanofluid suction/injection Reynolds number as shown in figure (3a)-(3b). As Re increases, both the fluid injected into the channel at the left permeable wall and the fluid sucked out of the channel at the right permeable wall increase, consequently, the heat transfer rate across the channel increases and the velocity profile decreases but skewed towards the right wall due to combine action of suction and axial pressure gradient. Moreover, both the entropy generation rate and the Bejan number decrease at the left wall region but increase at the right wall region as illustrated in figure (3c) – (3d). This may be attributed to the dominant effects of injection and fluid friction irreversibility at the left wall region, whereas at the right wall region, the heat transfer irreversibility and fluid suction dominate.

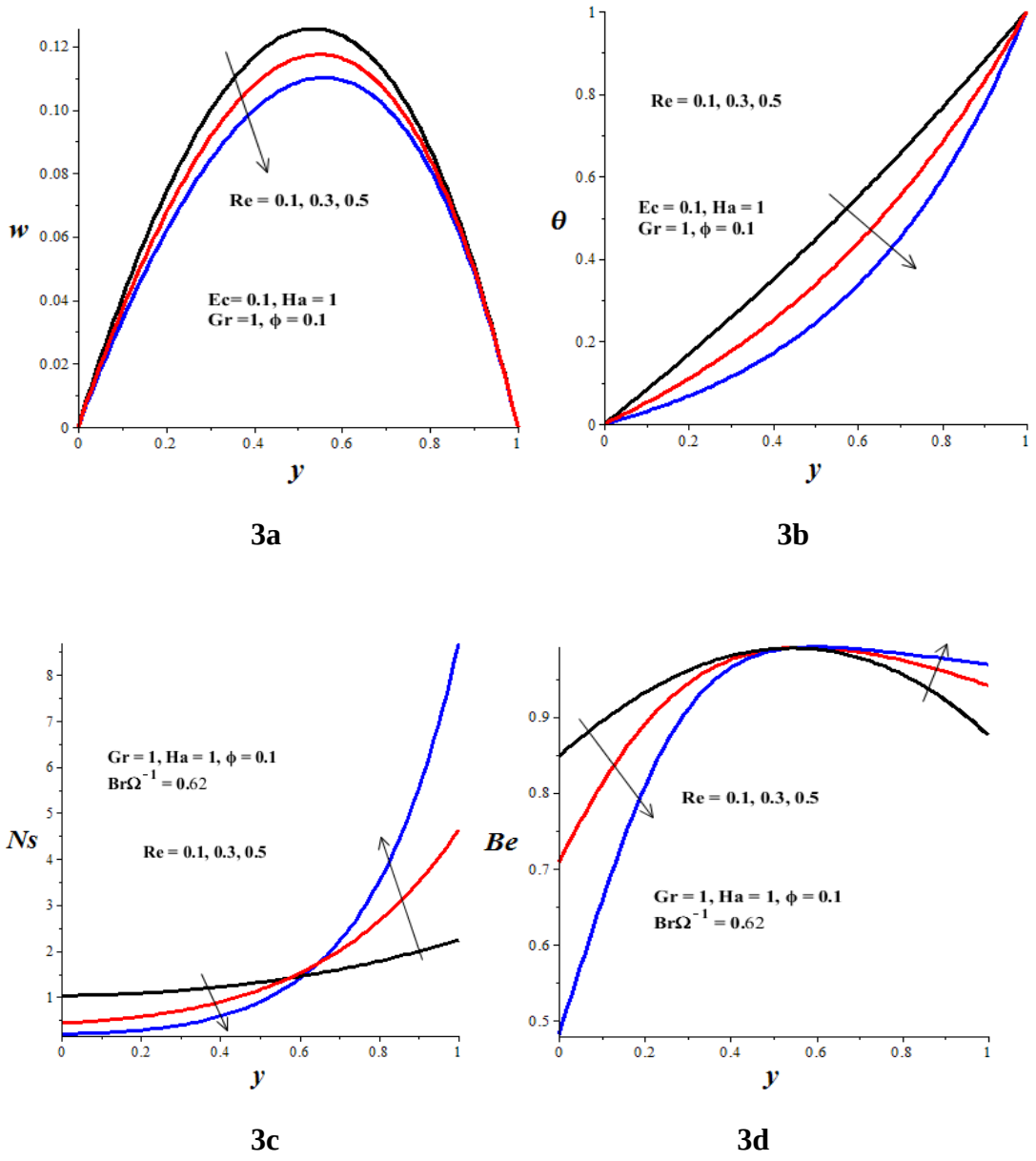

Figure 3: Effect of suction/injection Reynolds number on a) velocity, b) temperature c) entropy generation rate, d) Bejan number

Figures (4a)-(4c) represent the effects of increasing Grashof number (*Gr*) on the nanofluid velocity, temperature, entropy generation rate and Bejan number. With a rise in Grashof number, an up-thrust is encouraged within the vertical channel which ultimately enhances the nanofluid flow as illustrated in figure (4a). This also implies that inter-particle collision will be on the increase leading to an internal heat generation and a rise in the fluid temperature as shown in figure (4b). Meanwhile, the

entropy generation rate increases and the Bejan number decreases as illustrated in figures (4c) and (4d) with a rise in Grashof number. This implies that the fluid friction irreversibility strongly dominate the entropy production with increasing thermal buoyancy.

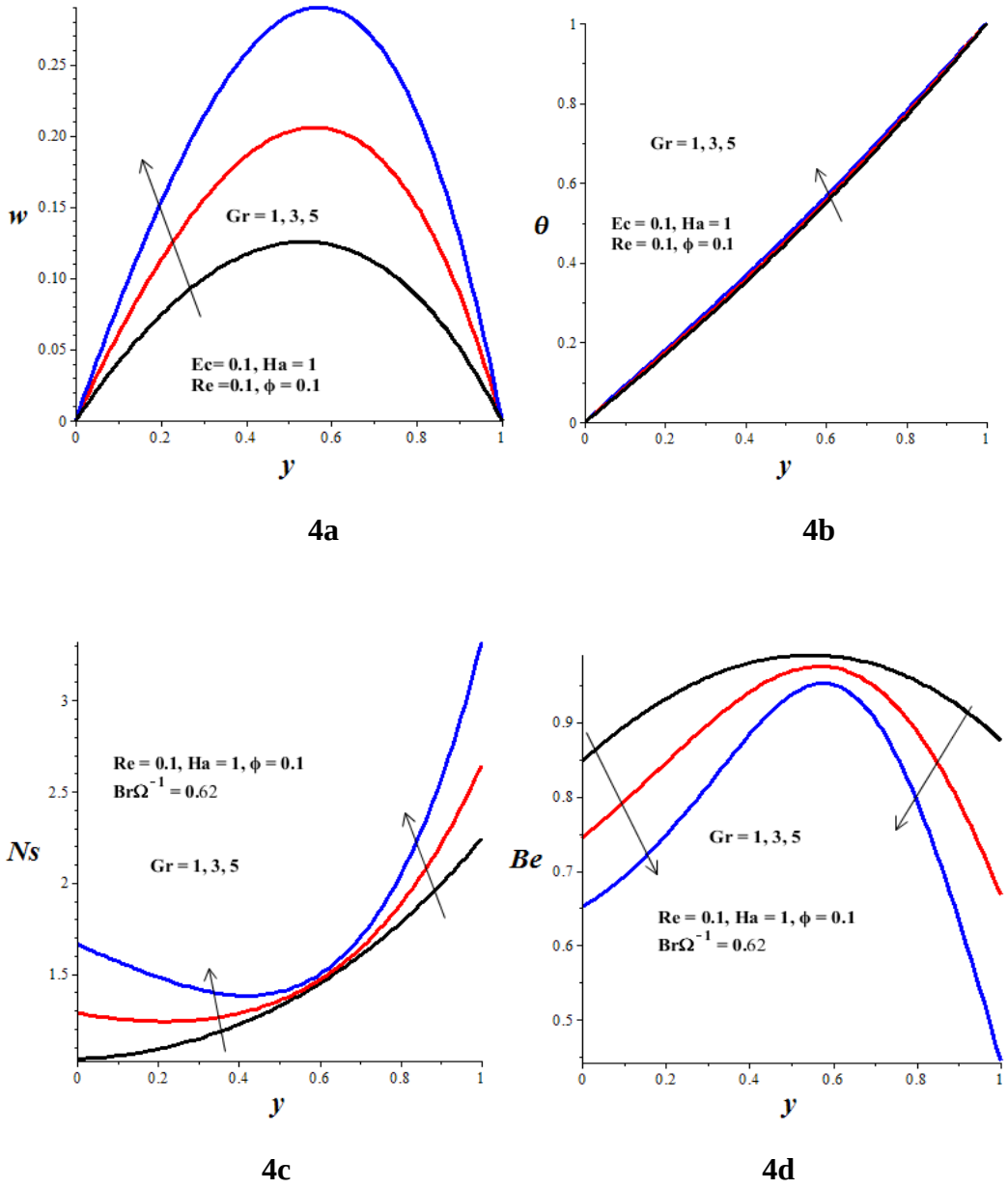

4a **4b**

4c **4d**

Figure 4: Effect of Grashof number on a) velocity, b) temperature c) entropy generation rate, d) Bejan number

The effects of increasing Hartmann number on the overall flow and thermal structure are demonstrated in figure (5). A rise in the magnetic field intensity decreases the velocity profiles across the channel due to resisting influence of the Lorentz force as shown in figure (5a). Meanwhile, the fluid temperature profiles in figure (5b) slightly decreases with a rise in magnetic field. This may be attributed to the combined effects on fluid suction and a rise in heat transfer rate with increasing magnetic field intensity leading to a decrease in fluid temperature. Interestingly, an increase in Hartmann number decreases the entropy production at the permeable walls region but increases the entropy production along the channel centreline region as depicted in figure (5c). The revise trend is observed in figure (5d) with increasing Bejan number at the permeable walls region and decreasing Bejan number around the channel core region. Consequently, as magnetic field intensity increases, heat transfer irreversibility dominates entropy production at the channel walls region while the effect of fluid friction irreversibility becomes prominent at the core of the channel.

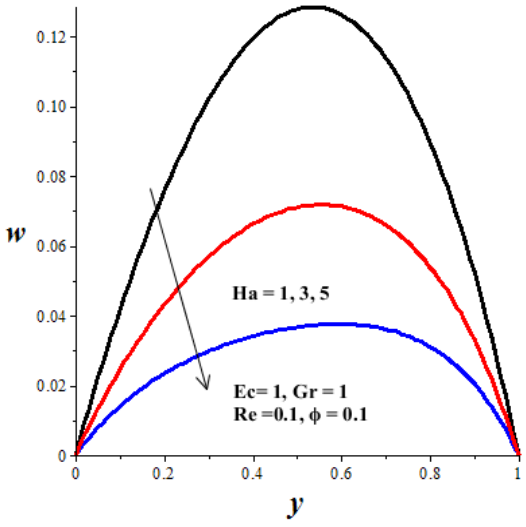

5a

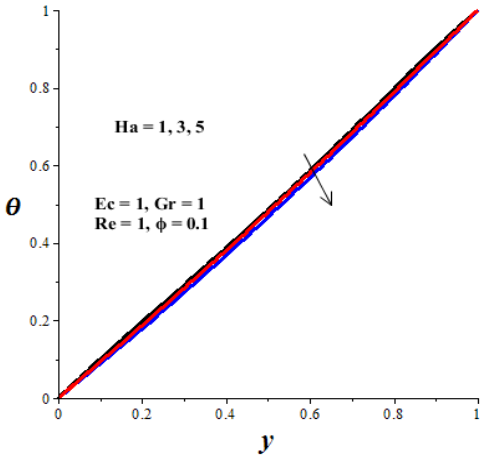

5b

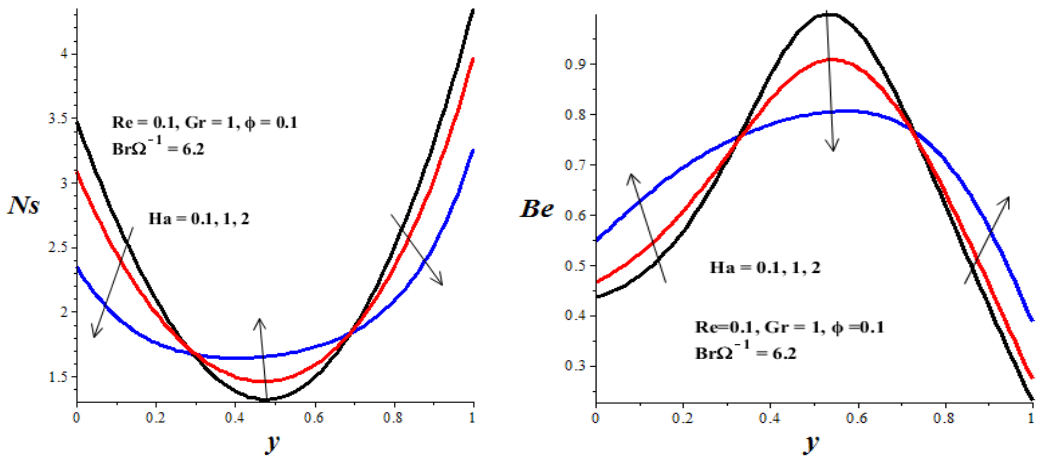

5c **5d**

Figure 5: Effect of Hartmann number on a) velocity, b) temperature c) entropy generation rate, d) Bejan number

In figures (6a)-(6d), the effects of Eckert number (*Ec*) and the group parameter ($Br\Omega^{-1}$) on the overall flow and thermal structure are presented. It is noteworthy that both the nanofluid velocity and temperature increase with an increase in Eckert number. As the parameter Ec increases, the combined effects of viscous and Joule heating increase, consequently, the fluid temperature increases and flow faster because the fluid becomes lighter as shown in figures (6a)–(6b). Meanwhile, an increase in the group parameter ($Br\Omega^{-1}$) enhances the entropy production but decreases the Bejan number as illustrated in figures (6c)-(6d). A rise in group parameter represents an increase in the effects of fluid friction irreversibility.

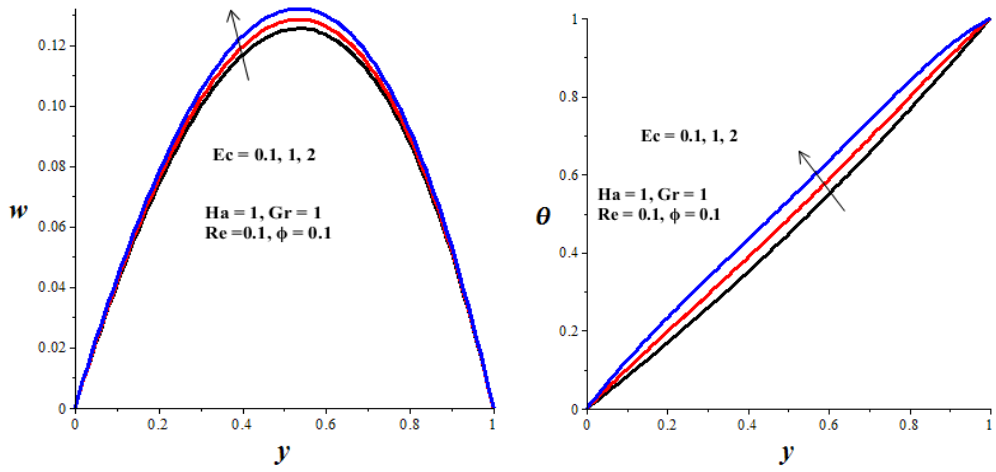

6a **6b**

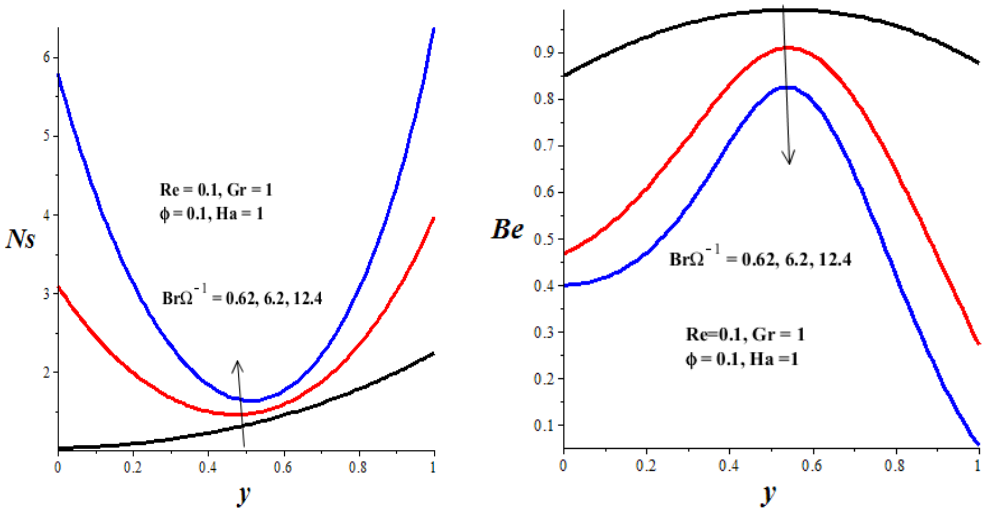

6c **6d**

Figure 6: Effect of Eckert number and Group parameter on a) velocity, b) temperature c) entropy generation rate, d) Bejan number

Figures (7a)-(7d) illustrate the effects of various thermophysical parameters on the skin friction and Nusselt number. As observed from the figures, the skin friction decreases with increasing values of *Ha* and ϕ but increases with an increase in *Ec*, *Gr* and *Re.* This can be attributed to a decrease or increase in nanofluid velocity gradient at the channel walls as the values of these parameters increases. Meanwhile, an increase in *Ec* and *Gr* decreases the Nusselt number due to a decrease in temperature gradient at the walls while an increase in *Ha*, ϕ and *Re* increases the Nusselt number due to an increase in temperature gradient at the walls.

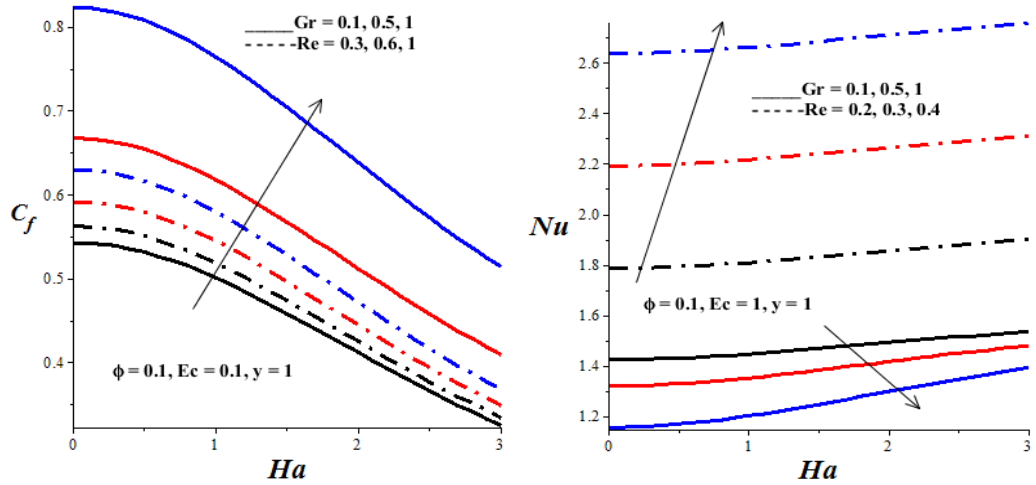

7a **7b**

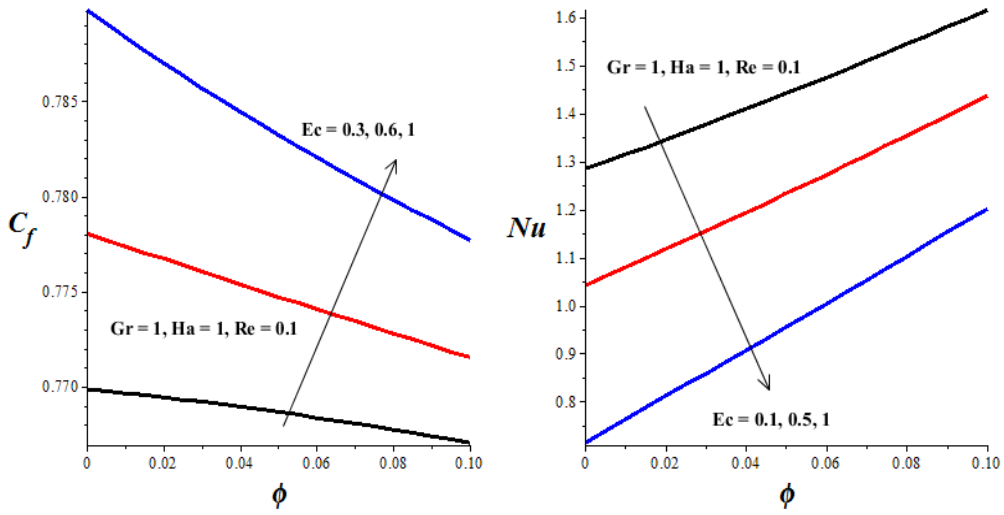

7c **7d**

Figure 7: Effect of parameter variation on skin friction and Nusselt number

5. CONCLUSION

Analysis is carried out for the entropy generation rate in hydromagnetic mixed convection flow of Cu-Water nanofluid through a channel with permeable wall. The velocity and the temperature profiles are obtained numerically using a fourth order Runge-Kutta-Fehlberg integration scheme. The skin friction, Nusselt number, entropy generation number with the Bejan number is computed.

The main results of present analysis are summarized below:

- The velocity profiles increases with *Gr* and *Ec* but decreases with *Re*, *Ha* and ϕ.
- The temperature profiles increases with *Ec*, *Gr*, and ϕ but decreases with Ha and Re.
- The skin friction increases with *Ec*, *Gr* and *Re* but decreases with *Ha* and ϕ.
- The Nusselt number increases with *Ha*, *Re* and ϕ but decreases with *Ec* and *Gr*.
- The entropy generation rate increases with *Gr*, ϕ and $Br\Omega^{-1}$. As *Re* increases, *Ns* decreases at the left wall region but increases at the right wall region. *Ns* at core region increases with *Ha* but decreases at the walls.
- The Bejan number decreases with *Gr*, ϕ and $Br\Omega^{-1}$ due to dominant effects of fluid friction irreversibility. As *Re* increases, *Be* decreases at the left wall region but increases at the right wall region. Moreover *Be* at core region decreases with *Ha* but increases at the walls.

The results obtained through this article shows that the optimal design and the efficient performance of a flow system involving nanofluid or a thermally designed system can be improved by choosing the appropriate values of the physical parameters. This will facilitate the reduction of entropy generated within the flow system.

REFERENCES

[1] T.G. Cowling, Magnetohydrodynamics, Interscience Publisher, Inc, New York, 1957.

[2] K.R. Cramer and S.I. Pai, Magnetofluid dynamics for engineers and applied physicists. McGraw-Hill, New York, 1973.

[3] S. U. S. Choi, Enhancing thermal conductivity of fluids with nanoparticles. ASME Fluids Eng Division 231 (1995) 99–105.

[4] J. Buongiorno, Convective transport in nanofluids. ASME J. Heat Transf. 128, (2006) 240-250.

[5] R. Saidur, K. Y. Leong, H. A. Mohammad, A review of applications and challenges of nanofluids. Renewable and Sustainable Energy Reviews 15 (2011) 1646-1668.

[6] O.D. Makinde, I. L. Animasaun, Bioconvection in MHD nanofluid flow with nonlinear thermal radiation and quartic autocatalysis chemical reaction past an upper surface of a paraboloid of revolution. International Journal of Thermal Sciences, 109 (2016) 159-171.

[7] S. M. Aminossadati, A. Raisi, B. Ghasemi, Effects of magnetic field on nanofluid forced convection in a partially heated microchannel. Int. J Non-Linear Mech, 46 (2011) 1373–1382.

[8] M. J. Uddin, W.A. Khan, A. I. Md. Ismail, Scaling group transformation for MHD boundary layer slip flow of a nanofluid over a convectively heated stretching sheet with heat generation. Mathematical problems in Engineering, Vol. 2012, article ID 934964, 2012.

[9] A. Bejan, A study of entropy generation in fundamental convective heat transfer. J. Heat Transf. 101(1979), 718-725.

[10] L. C. Woods, Thermodynamics of Fluid Systems. Oxford University Press, Oxford, UK; 1975.

[11] M.H. Mkwizu, O.D. Makinde: Entropy generation in a variable viscosity channel flow of nanofluid with convective cooling: Comptes Rendus Mécanique, Vol. 343, 38-56, 2015.

[12] S. Das, S. Chakraborty, R. N. Jana, O. D. Makinde, Entropy analysis of unsteady magneto-nanofluid flow past accelerating stretching sheet with

convective boundary condition. Applied Mathematics and Mechanics, Vol. 36, Issue 12, 1593-1610, 2015.

[13] S. O. Adesanya, O. D. Makinde, Irreversibility analysis in a couple stress film flow along an inclined heated plate with adiabatic free surface. Phys A 2015, 432, 222-229.

[14] S. O. Adesanya, O. D. Makinde, Entropy generation in couple stress fluid flow through porous channel with fluid slippage. International Journal of Exergy 2014, 15,344-362.

[15] S. Das, A.S. Banu, R.N. Jana, O.D. Makinde, Entropy analysis on MHD pseudo-plastic nanofluid flow through a vertical porous channel with convective heating. Alexandria Engineering Journal, Vol. 54(3), 325-337, 2015.

[16] C. C. Cho, Heat transfer and entropy generation of natural convection in nanofluid-filled square cavity with partially-heated wavy surface, International Journal of Heat & Mass Transfer 77 (4) (2014) 818-827.

[17] K. Y. Leong, R. Saidur, M. Khairulmaini, Heat transfer and entropy analysis of three different types of heat exchangers operated with nanofluids. International Communications in Heat & Mass Transfer 39 (6) (2012) 838-843.

[18] A. H. Mahmoudi, I. Pop, M. Shahi, F. Talebi, MHD natural convection and entropy generation in a trapezoidal enclosure using Cu–water nanofluid. Computers & Fluids 72 (2013) 46–62.

[19] H. C. Brinkman, The viscosity of concentrated suspensions and solutions. J. Chem. Phys. 20 (1952) 571–581.

[20] J. C. Maxwell, A treatise on electricity and magnetism. 2nd ed. Cambridge: Oxford University Press; (1904), 435–441.

[21] J. H. Ferziger, M. Peric, Computational method for fluid dynamics. New York: Springer Verlag, 1999.